

# Multi-wavelength interferometry of evolved stars using VLTI and VLBA

M. Wittkowski<sup>1</sup>, D. A. Boboltz<sup>2</sup>, T. Driebe<sup>3</sup>, and K. Ohnaka<sup>3</sup>

<sup>1</sup> European Southern Observatory, Garching, Germany [mwittkow@eso.org](mailto:mwittkow@eso.org)

<sup>2</sup> U.S. Naval Observatory, Washington, DC, USA [dboboltz@usno.navy.mil](mailto:dboboltz@usno.navy.mil)

<sup>3</sup> Max-Planck-Institut für Radioastronomie, Bonn, Germany  
[driebe@mpifr-bonn.mpg.de](mailto:driebe@mpifr-bonn.mpg.de), [kohnaka@mpifr-bonn.mpg.de](mailto:kohnaka@mpifr-bonn.mpg.de)

**Summary.** We report on our project of coordinated VLTI/VLBA observations of the atmospheres and circumstellar environments of evolved stars. We illustrate in general the potential of interferometric measurements to study stellar atmospheres and envelopes, and demonstrate in particular the advantages of a coordinated multi-wavelength approach including near/mid-infrared as well as radio interferometry. We have so far made use of VLTI observations of the near- and mid-infrared stellar sizes and of concurrent VLBA observations of the SiO maser emission. To date, this project includes studies of the Mira stars S Ori and RR Aql as well as of the supergiant AHSco. These sources all show strong silicate emission features in their mid-infrared spectra. In addition, they each have relatively strong SiO maser emission. The results from our first epochs of S Ori measurements have recently been published [5] and the main results are reviewed here. The S Ori maser ring is found to lie at a mean distance of about 2 stellar radii, a result that is virtually free of the usual uncertainty inherent in comparing observations of variable stars widely separated in time and stellar phase. We discuss the status of our more recent S Ori, RR Aql, and AHSco observations, and present an outlook on the continuation of our project.

## 1 Introduction

The evolution of cool luminous stars, including Mira variables, is accompanied by significant mass-loss to the circumstellar environment (CSE) with mass-loss rates of up to  $10^{-7} - 10^{-4} M_{\odot}/\text{year}$  (e.g. [18]). The detailed structure of the CSE, the detailed physical nature of the mass-loss process from evolved stars, and especially its connection with the pulsation mechanism in the case of Mira variable stars, are not well understood. Furthermore, one of the basic unknowns in the study of late-type stars is the mechanism by which usually spherically symmetric stars on the asymptotic giant branch (AGB) evolve to form axisymmetric or bipolar planetary nebulae (PNe). Possible origins of asymmetric structures include, among others, binarity, capture of substellar companions, stellar rotation, or magnetic fields. While it is generally believed that the observed pronounced asymmetries of the envelopes of PNe form when the star evolves from the tip of the AGB branch toward the blue part of the HR diagram, there is evidence for some asymmetric structures already around AGB stars and supergiants (e.g., [27, 28, 29, 21, 4]).

Coordinated multi-wavelength studies (near-infrared, mid-infrared, radio, millimeter) of the stellar surface (photosphere) *and* the CSE at different distances

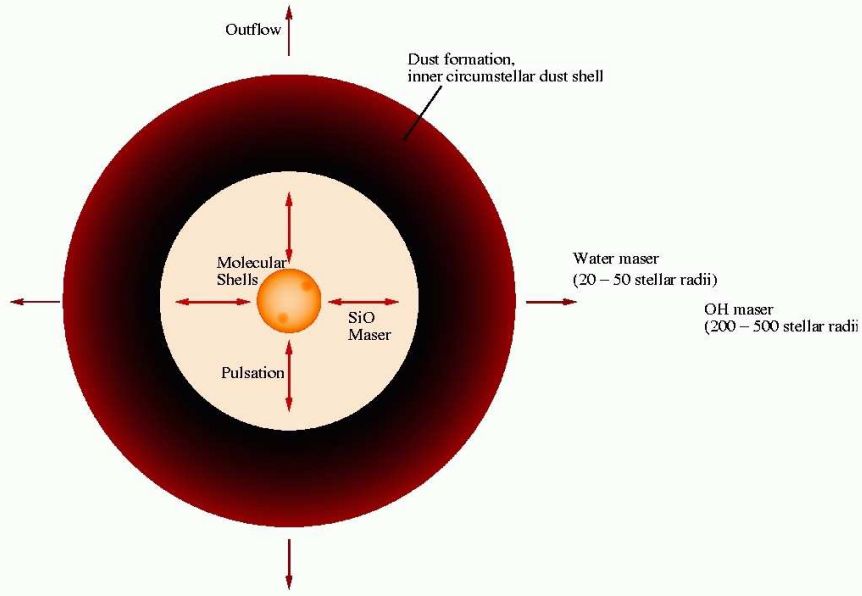


**Fig. 1.** Sketch of a Mira variable star and its circumstellar envelope (CSE). A multi-wavelength study (MIDI/AMBER/VLBA) is well suited to probe the different regions shown here. Owing to the stellar variability, only contemporaneous observations are meaningful.

from the stellar photosphere and obtained at corresponding cycle/phase values of the stellar variability curve are best suited to improve our general understanding of the atmospheric structure, the CSE, the mass-loss process, and ultimately of the evolution of symmetric AGB stars toward axisymmetric or bipolar planetary nebulae. Fig. 1 shows a schematic view of a Mira variable star, indicating the different regions that can be probed by different techniques/wavelength ranges (VLTI/AMBER, VLTI/MIDI, VLBA/maser, ALMA). Fig. 2 shows a comparison of the VLTI, VLBA, ALMA, and VLA interferometric facilities in terms of wavelength ranges and angular resolution. VLTI, VLBA, and ALMA allow us to observe the same evolved stars in terms of sensitivity, and reach a comparable angular resolution at their respective wavelength ranges.

The conditions near the stellar surface can best be studied by means of optical/near-infrared long-baseline interferometry. This technique has provided information regarding the stellar photospheric diameter, asymmetries/surface inhomogeneities, effective temperature, and center-to-limb intensity variations including the effects of close molecular shells, for a number of non-Mira and Mira giants (see, e.g., [12, 30, 26, 15, 32, 33, 5, 9]).

The structure and physical parameters of the molecular shells located between the photosphere and the dust formation zone, as well as of the dust shell itself can be probed by mid-infrared interferometry (e.g. [7]). This has also recently been demonstrated by using the spectro-interferometric capabilities of the VLTI/MIDI

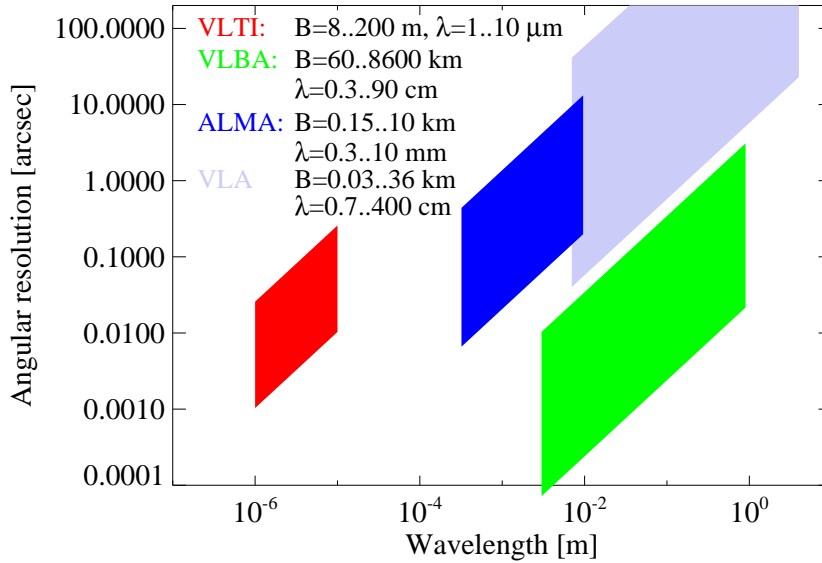


**Fig. 2.** Comparison of resolution and wavelength ranges of the infrared, millimeter, and radio interferometric facilities VLTI, ALMA, VLBA, and VLA.

instrument to study the Mira star RR Sco [22]. The model obtained in this work includes a warm molecular (SiO and H<sub>2</sub>O) layer as well as a dust shell of corundum and silicate, and can well reproduce the obtained MIDI visibility values.

Complementary information regarding the molecular shells can be obtained by observing the maser radiation that some of these molecules emit. The structure and dynamics of the CSE of Mira variables and other evolved stars has been investigated by mapping SiO maser emission at typically about 2 stellar radii toward these stars using very long baseline interferometry (VLBI) at radio wavelengths (e.g., [3, 19, 5]).

Results regarding the relationships between the different regions mentioned above and shown in Fig. 1 suffer often from uncertainties inherent in comparing observations of variable stars widely separated in time and stellar phase (see the discussion in [5]). Both, the photospheric stellar size as well as the mean diameter of the SiO maser shell are known to vary as a function of the stellar variability phase with amplitudes of 20-50% (see [17] for theoretical and [26] for observational estimates of the variability of the stellar diameter; as well as [16] for theoretical and [8] for observational estimates of the variability of the mean SiO maser ring diameter).

To overcome these limitations, we have established a program of coordinated and concurrent observations at near-infrared, mid-infrared, and radio wavelengths of evolved stars, aiming at a better understanding of the structure of the CSE, of the mass-loss process, and of the triggering and formation of asymmetric structures.

In the following, we describe recent results obtained with optical/infrared interferometry on the stellar atmospheric structure of regular non-Mira (Section 2) and Mira (Section 3) giants. Our joint VLTI/VLBA observations of the Mira star

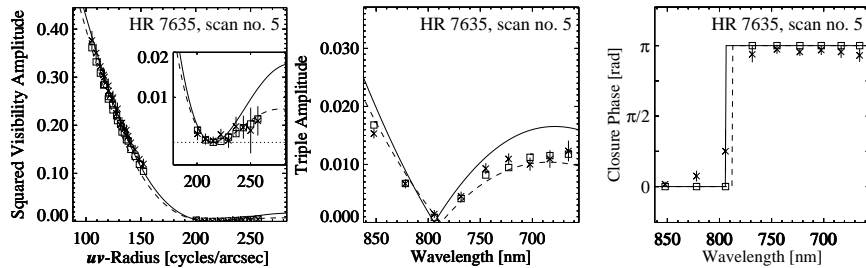


**Fig. 3.** NPOI limb-darkening observations (squared visibility amplitude, triple amplitude, closure phase) of the M0 giant  $\gamma$ Sge, together with a comparison to the best fitting ATLAS 9 model atmosphere prediction (squares). For comparison, the solid line denotes a uniform disk model, and the dashed line a fully-darkened disk model. ATLAS 9 models with variations of  $T_{\text{eff}}$  and  $\log g$  result in significantly different model predictions. From [30].

S Ori are discussed in Section 4. Finally, we give an outlook (Section 5) on further measurements and future ideas. The latter includes desirable 2nd generation instrumentation based on the requirements of this particular project alone.

## 2 The atmospheric structure of non-Mira giants

Fundamental parameters, most importantly radii and effective temperatures, of regular cool giant stars have frequently been obtained with interferometric and other high angular resolution techniques, thanks to the favorable brightness and size of these stars. Further parameters of the stellar structure, as the strength of the limb-darkening effect, can be studied when more than one resolution element across the stellar disk is employed. Through the direct measurement of the center-to-limb intensity variation (CLV) across stellar disks and their close environments, interferometry probes the vertical temperature profile, as well as horizontal inhomogeneities. However, the required direct measurements of stellar intensity profiles are among the most challenging programs in modern optical interferometry. Since more than one resolution element across the stellar disk is needed to determine surface structure parameters beyond diameters, the long baselines needed to obtain this resolution also produce very low visibility amplitudes corresponding to vanishing fringe contrasts. Such direct limb-darkening studies have been accomplished for a relatively small number of stars using different interferometric facilities (including, for instance, [11, 23, 10, 30, 32]).

Recent optical multi-wavelength measurements of the cool giants  $\gamma$ Sge and BY Boo [30] succeeded not only in directly detecting the limb-darkening effect, but also in constraining ATLAS 9 ([20]) model atmosphere parameters. Fig. 3 shows one dataset including squared visibility amplitudes, triple amplitudes, and closure phases of the M0 giant  $\gamma$ Sge obtained with NPOI, together with a comparison to the best fitting ATLAS 9 model atmosphere prediction. ATLAS 9 models with variations of  $T_{\text{eff}}$  and  $\log g$  result in significantly different model predictions. By this

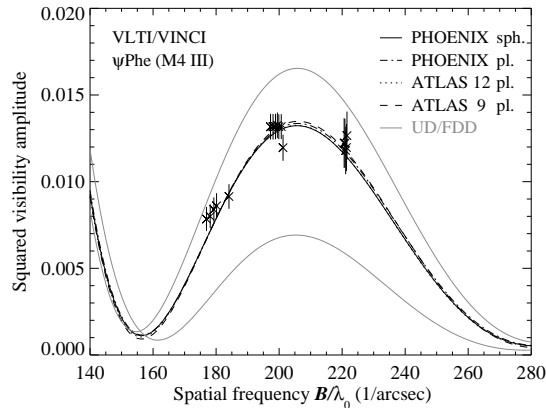


**Fig. 4.** VLTI limb-darkening observations of the M4 giant  $\psi$  Phe [32].

direct comparison of the NPOI data to the **ATLAS 9** models alone, the effective temperature of  $\gamma$  Sge is constrained to  $4160 \pm 100$  K. The limb-darkening observations are less sensitive to variations of the surface gravity, and  $\log g$  is constrained to  $0.9 \pm 1.0$  [30]. These constraints are well consistent with independent estimates, such as calibrations of the spectral type. Furthermore, it was shown that these interferometric and spectroscopic measurements of  $\gamma$  Sge both compare well with predictions by the same spherical **PHOENIX** [13] model atmosphere [2].

The first limb-darkening observation that was obtained with the VLTI succeeded in the early commissioning phase of the VLTI [32]. Using the VINCI instrument,  $K$ -band visibilities of the M4 giant  $\psi$  Phe were measured in the first and second lobe of the visibility function. These observations were found to be consistent with predictions by **PHOENIX** and **ATLAS** model atmospheres, the parameters for which were constrained by comparison to available spectrophotometry and theoretical stellar evolutionary tracks (see Fig. 4). Such limb-darkening observations also result in very precise and accurate radius estimates because of the precise description of the CLV. Future use of the spectro-interferometric capabilities of **AMBER** and **MIDI** will enable us to study the wavelength-dependence of the limb-darkening effect, which results in stronger tests and constraints of the model atmospheres than these broad-band observations (cf. the wavelength-dependent optical studies with NPOI as described above).

Another strong test of model atmospheres is the direct comparison of spectrophotometry, high-resolution spectra, and limb-darkening observations to predictions by the same model atmosphere. Such studies are presented in these proceedings (V. Roccatagliata et al.). Available spectrophotometry, high-resolution UVES ultraviolet/optical spectra, as well as near-infrared VLTI/VINCI  $K$ -band limb-darkening measurements are compared to predictions by **PHOENIX** model atmospheres, and good agreement is found (see Figs. 1 and 2 in Roccatagliata et al., these proceedings).

### 3 The atmospheric structure of Mira giants

For cool pulsating Mira stars, the CLVs are expected to be more complex than for non-pulsating M giants due to the effects of molecular layers close to the continuum-forming layers. Based on self-excited hydrodynamic model atmospheres of Mira stars ([14, 25, 17], Scholz & Wood, private communication), broad-band CLVs may indeed appear as Gaussian-shaped or multi-component functions, and to exhibit temporal variations as a function of stellar phase and cycle, in accordance with observations (see introduction). These complex shapes of the CLV make it difficult to define an appropriate stellar radius. Different radius definitions, such as the Roseland mean radius, the continuum radius, or the radius at which the filter-averaged intensity drops by 50%, may result in different values for the same CLV. For complex CLVs at certain variability phases these definitions can result in differences of up to about 20% (on these topics, see also [24]). However, interferometric measurements covering a sufficiently wide range of spatial frequencies can directly be compared to CLV predictions by model atmospheres without the need of a particular radius definition. At pre-maximum stellar phases, when the temperature is highest, the broad-band CLVs are less contaminated by molecular layers, and different radius definitions agree relatively well (Scholz & Wood, private communication).

*K*-band VINCI observations of the prototype Mira stars *o*Cet and R Leo have been presented by [33] and [9], respectively. These measurements are also described in more detail elsewhere in these proceedings (Driebe et al., Fedele et al.). These measurements at post-maximum stellar phases indicate indeed *K*-band CLVs which are clearly different from a uniform disk profile already in the first lobe of the visibility function. The measured visibility values were found to be consistent with predictions by the self-excited dynamic Mira model atmospheres described above that include molecular shells close to continuum-forming layers.

### 4 Joint VLTI/VLBA observations of the Mira star S Ori

We started our project of joint VLTI/VLBA observations of Mira stars in December 2002/January 2003 with coordinated near-infrared *K*-band VLTI/VINCI observations of the stellar diameter of the Mira variable S Ori and quasi-simultaneous VLBA observations of the 43.1 GHz and 42.8 GHz SiO maser emissions toward this star [5]. We obtained in December 2004/January 2005 further concurrent observations including mid-infrared VLTI/MIDI observations to probe the molecular layers and the dust shell of S Ori, and new epochs of VLBA observations of the 43.1 GHz and 42.8 GHz SiO maser rings.

The December 2002/January 2003 observations represent the first-ever coordinated observations between the VLTI and VLBA facilities, and the results from these observations were recently published [5]. Analysis of the SiO maser data recorded at a visual variability phase 0.73 show the average distance of the masers from the center of the distribution to be 9.4 mas for the  $v = 1, J = 1 - 0$  (43.1 GHz) masers and 8.8 mas for the  $v = 2, J = 1 - 0$  (42.8 GHz) masers. The velocity structure of the SiO masers appears to be random with no significant indication of global expansion/infall or rotation. The determined near-infrared, *K*-band, uniform disk (UD) diameters decreased from  $\sim 10.5$  mas at phase 0.80 to  $\sim 10.2$  mas

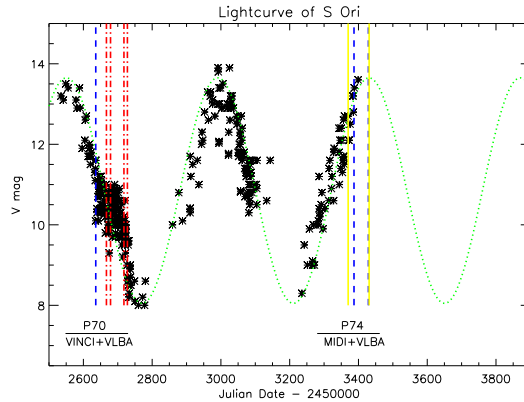


**Fig. 5.** Lightcurve of S Ori together with the epochs of our joint VLTI/VLBA measurements obtained so far. Note that the y-axis is given with increasing  $V$  magnitude, i.e. the stellar maximum is at the bottom and stellar minimum at the top. The study of S Ori was started in ESO period P70 (Dec. 2002/Jan. 2003) including near-infrared  $K$ -band VINCI and VLBA/SiO maser observations [5]. In December 2004/January 2005, we obtained concurrent mid-infrared VLTI/MIDI and VLBA/SiO maser observations.

at phase 0.95. For the epoch of our VLBA measurements, an extrapolated UD diameter of  $\Theta_{\text{UD}}^K = 10.8 \pm 0.3$  mas was obtained, corresponding to a linear radius of  $R_{\text{UD}}^K = 2.3 \pm 0.5$  AU or  $R_{\text{UD}}^K = 490 \pm 115 R_{\odot}$ . The model predicted difference between the continuum and  $K$ -band UD diameters is relatively low in the pre-maximum region of the visual variability curve as in the case of our observations (see above). At this phase of 0.73, the continuum diameter may be smaller than the  $K$ -band UD diameter by about 15% [17]. With this assumption, the continuum photospheric diameter for the epoch of our VLBA observation would be  $\Theta_{\text{Phot}}(\text{VLBA epoch, phase} = 0.73) \approx 9.2$  mas. Our coordinated VLBA/VLTI measurements show that the masers lie relatively close to the stellar photosphere at a distance of  $\sim 2$  photospheric radii, consistent with model estimates [16] and observations of other Mira stars [6]. This result is virtually free of the usual uncertainty inherent in comparing observations of variable stars widely separated in time and stellar phase.

The new 2004/2005 VLTI and VLBA data are currently being reduced and analyzed.

## 5 Outlook

We are concentrating on a few stars in order to understand the CSE for a few sources in depth. In addition to the S Ori data described above, we have to date VLTI/MIDI observations of the supergiant AHSco (Jul. 2005, Aug. 2005), and of the Mira star RR Aql (Jul. 2005, Aug. 2005), as well as concurrent VLBA observations for each of these targets/epochs. These data are currently being analyzed. There may be

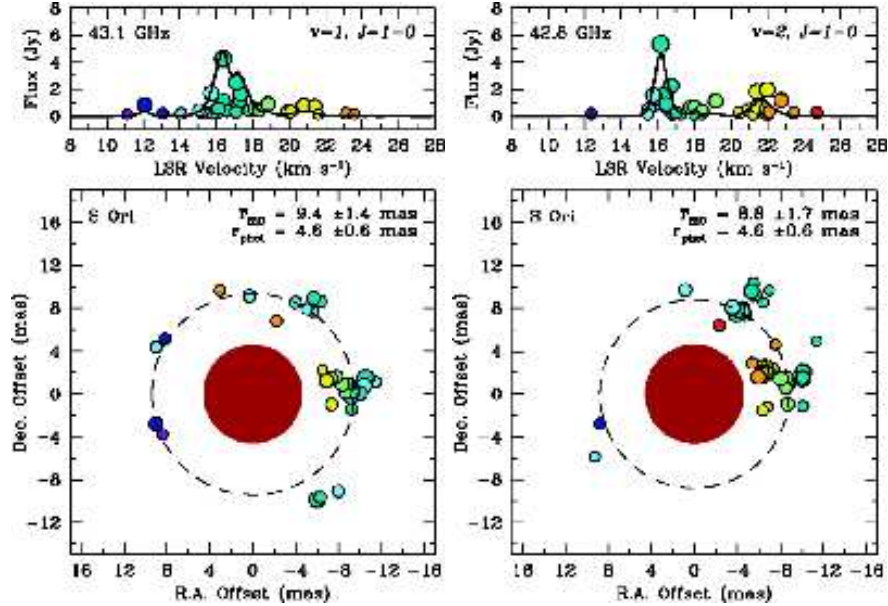


**Fig. 6.** First-ever coordinated observations between ESO’s VLTI and NRAO’s VLBA facilities: SiO maser emissions toward the Mira variable S Ori measured with the VLBA, together with the near-infrared diameter measured quasi simultaneously with the VLTI (red stellar disk). The left panels shows the 43.1 GHz maser transition, and the right panel the 42.8 GHz transition. From [5].

hints toward an inherent difference in the structure between Mira variables and supergiants, in particular regarding the relative distances of photosphere, SiO maser ring, and inner dust shell boundary (cf. [7, 5]).

Further studies will aim at including more detailed near-infrared studies of the stellar atmospheric structure (close to the photosphere) employing VLTI/AMBER, concurrent with VLTI/MIDI and VLBA observations as discussed above. Making use of the spectro-interferometric capabilities of AMBER, and also of the closure-phase information, these studies can in principle also reveal horizontal surface inhomogeneities (see, e.g. [31]).

A further step toward our better understanding of the stellar mass-loss process are interferometric measurements of post-AGB stars. The first detection of the envelope which surrounds the post-AGB binary source HR 4049, by *K*-band VINCI observations, was recently reported by [1]. A physical size of the envelope in the near-infrared *K*-band of about 15 AU (Gaussian FWHM) was derived. These measurements provide information on the geometry of the emitting region and cover a range of position angles of about 60 deg. They show that there is only a slight variation of the size with position angle covered within this range. These observations are, thus, consistent with a spherical envelope at this distance from the stellar source, while an asymmetric envelope cannot be completely ruled out due to the limitation in azimuth range, spatial frequency, and wavelength range. Further

investigations using the near-infrared instrument AMBER can reveal the geometry of this near-infrared component in more detail, and MIDI observations can add information on cooler dust at larger distances from the stellar surface.

In the more distant future, when second generation instruments at the VLTI become available, a very valuable addition and continuation of this project would be an improved imaging capability of the VLTI, both at near-infrared as well as at mid-infrared wavelengths. This would enable us to detect and correlate asymmetric structures at the stellar surface and dust shell in a much more precise way, and hence to better understand the transition from spherically symmetric AGB stars to axisymmetric or bipolar planetary nebulae. Improved imaging capabilities can be reached by an increased number of simultaneously combined beams. Furthermore, an improved spatial resolution (by using longer baselines) would be desirable to better match the high angular resolution of the VLBA.

## References

1. S. Antonucci, F. Paresce, & M. Wittkowski: *A&A* **429**, L1 (2005)
2. J. P. Aufdenberg, & P. H. Hauschildt: *Proc. SPIE* **4838**, 193 (2003)
3. D. A. Boboltz, P. J. Diamond, & A. J. Kemball: *ApJ* **487**, L147 (1997)
4. D. A. Boboltz, & P. J. Diamond: *AAS* **197**, 4507 (2000)
5. D. A. Boboltz, & M. Wittkowski: *ApJ* **618**, 953 (2005)
6. W. D. Cotton, B. Mennesson, P. J. Diamond, et al.: *A&A* **414**, 275
7. W. C. Danchi, M. Bester, C. G. Degiacomi, et al.: *AJ* **107**, 1469 (1994)
8. P. J. Diamond, & A. J. Kemball: *ApJ* **599**, 1372 (2003)
9. D. Fedele, M. Wittkowski, F. Paresce, et al.: *A&A* **431**, 1019 (2005)
10. A. R. Hajian, J. T. Armstrong, C. A. Hummel et al.: *ApJ* **496**, 484 (1998)
11. R. Hanbury Brown, et al.: *MNRAS* **167**, 475 (1973)
12. C. A. Haniff, M. Scholz, & P. G. Tuthill: *MNRAS* **276**, 640 (1995)
13. P. H. Hauschildt, F. Allard, J. Ferguson, et al.: *ApJ* **525**, 871 (1999)
14. K.-H. Hofmann, M. Scholz, & P. R. Wood: *A&A* **339**, 846 (1998)
15. K.-H. Hofmann, U. Beckmann, T. Blöcker, et al.: *New Astronomy* **7**, 9 (2002)
16. E. M. L. Humphreys, M. D. Gray, J. A. Yates, et al.: *A&A* **386**, 256 (2002)
17. M. J. Ireland, M. Scholz, & P. R. Wood: *MNRAS* **352**, 318 (2004)
18. M. Jura, & S. G. Kleinmann: *ApJS* **73**, 769 (1990)
19. A. J. Kemball, & P. J. Diamond: *ApJ* **481**, L111 (1997)
20. R. Kurucz: *Kurucz CD-ROM No. 17.*, Cambridge, Mass. (1993)
21. J. D. Monnier, P. G. Tuthill, B. Lopez, et al.: *ApJ* **512**, 351 (1999)
22. K. Ohnaka, J. Bergeat, T. Driebe, et al.: *A&A* **429**, 1057 (2005)
23. A. Quirrenbach, D. Mozurkewich, D. F. Buscher, et al.: *A&A* **312**, 160 (1996)
24. M. Scholz: *Proc. SPIE* **4838**, 163 (2003)
25. A. Tej, A. Lancon, M. Scholz, & P. R. Wood: *A&A* **412**, 481 (2003)
26. R. R. Thompson, M. J. Creech-Eakman, & R. L. Akeson: *ApJ* **570**, 373 (2002)
27. G. Weigelt, Y. Balega, K.-H. Hofmann, & M. Scholz: *A&A* **316**, L21 (1996)
28. G. Weigelt, Y. Balega, T. Blöcker, et al.: *A&A* **333**, L51 (1998)
29. M. Wittkowski, N. Langer, G. Weigelt: *A&A* **340**, L39 (1998)
30. M. Wittkowski, C. A. Hummel, K. J. Johnston, et al.: *A&A* **377**, 981 (2001)
31. M. Wittkowski, M. Schöller, S. Hubrig, et al.: *AN* **323**, 241 (2002)
32. M. Wittkowski, J. P. Aufdenberg, & P. Kervella: *A&A* **413**, 711 (2004)
33. H. C. Woodruff, M. Eberhardt, T. Driebe, et al.: *A&A* **421**, 703 (2004)